MEDDOCS Open Access Publisher

ISSN: 2690-4004

Journal of Clinical Images

Open Access | Research Article

Diffusion Weighted Imaging and Intravoxel Incoherent Motion Magnetic Resonance Imaging are Potential Lenvatinib Treatment Response Biomarkers for Advanced Hepatocellular Carcinoma

Yu Zhang[1]; Satoshi Kobayashi[1,2]; Azusa Kitao[1*]; Yudai Shogan[3]; Naoki Ohno[4]; Noboru Takata[5]; Takeshi Terashima[5]; Kuniaki Arai[5]; Tatsuya Yamashita[5]; Taro Yamashita[5]; Norihide Yoneda[1]; Kazuto Kozaka[1]; Toshifumi Gabata[1]*

[1]*Department of Radiology, Kanazawa University Graduate School of Medical Science, Japan.*

[2]*Department of Quantum Medical Technology, Kanazawa University Graduate School of Medical Science, Japan.*

[3]*Department of Radiological Technology, Kanazawa University Hospital, Japan.*

[4]*Faculty of Health Sciences, Institute of Medical, Pharmaceutical and Health Sciences, Kanazawa University, Japan.*

[5]*Department of Gastroenterology, Kanazawa University Graduate School of Medical Science, Japan.*

***Corresponding Authors:**

Satoshi Kobayashi & Azusa Kitao

Department of Radiology, Kanazawa University Graduate School of Medical Science, 13-1 Takaramachi, Kanazawa 920-8640, Japan.

Email: satoshik@staff.kanazawa-u.ac.jp & kitaoa@staff.kanazawa-u.ac.jp

Received: Jul 01, 2023

Accepted: Jul 18, 2023

Published Online: Jul 25, 2023

Journal: Journal of Clinical Images

Publisher: MedDocs Publishers LLC

Online edition: http://meddocsonline.org/

Keywords: Diffusion weighted imaging; Intravoxel incoherent motion; Hepatocellular carcinoma; Lenvatinib.

Abbreviations: ADC: Apparent Diffusion Coefficient; DWI: Diffusion-Weighted Imaging; DC: True Diffusion Coefficient; D*: Pseudo Diffusion Coefficient; ER: Enhancement Ratio, HCC: Hepatocellular Carcinoma; IVIM: Intravoxel Incoherent Motion; MRI: Magnetic Resonance Imaging; PD: Progressive Disease; PF: Perfusion Fraction.

Abstract

Purpose: To evaluate associations between the therapeutic outcomes of lenvatinib for advanced Hepatocellular Carcinoma (HCC), and Diffusion Weighted Imaging (DWI) and Intravoxel Incoherent Motion (IVIM) Magnetic Resonance Imaging (MRI) parameters.

Methods: We included 16 patients who underwent lenvatinib therapy for advanced HCC from March to October 2019 and then compared the DWI/IVIM parameters and enhancement ratios in the arterial phase of gadoxetate enhanced T1 weighted images between those with and without Progressive Disease (PD) at baseline and two and six weeks after treatment. We also compared the DWI/IVIM parameters between viable, hemorrhagic, and necrotic tumor tissue areas. Finally, the baseline DWI/IVIM parameters and enhancement ratios were used to generate receiver operating characteristic curves for predicting PD.

Results: At baseline, the non-PD group had significantly lower apparent diffusion coefficient (ADC) and true diffusion coefficient (DC) values than the PD group (ADC: P=0.007; DC: P=0.018). Furthermore, the non-PD group had significantly increased ADC and DC values after six weeks than at baseline (ADC: P <0.001; DC: P=0.003). The ADC and DC values were significantly higher in necrotic areas than in viable areas after six weeks (both P <0.001). In contrast, the values were significantly lower in hemorrhagic areas than in viable

Cite this article: Zhang Y, Kobayashi S, Kitao A, Shogan Y, Ohno N, et al. Diffusion Weighted Imaging and Intravoxel Incoherent Motion Magnetic Resonance Imaging are Potential Lenvatinib Treatment Response Biomarkers for Advanced Hepatocellular Carcinoma. J Clin Images. 2023; 6(2): 1145.

areas (both P <0.001). The ADC and DC cutoff values were 1.191 (10^{-3} mm^2/s; Area Under the Curve [AUC] =0.825, 95% confidence interval [CI]: 0.596, 1.000) and 0.986 (10^{-3} mm^2/s; AUC=0.865, 95% CI: 0.684, 1.000), respectively.

Conclusion: ADC and DC help predict the therapeutic outcomes of lenvatinib for advanced HCC.

Introduction

Hepatocellular Carcinoma (HCC) is seventh most frequently occurring cancer in the world and the second most common cause of cancer mortality [1]. Various drugs have been developed to improve the survival rate of patients with advanced HCC, especially in recent years. For example, lenvatinib, a multikinase inhibitor, prolongs the median survival and time to progression in patients with advanced HCC [2]. Lenvatinib inhibits tumor cell proliferation and angiogenesis by blocking the Fibroblast Growth Factor Receptor (FGFR), Vascular Endothelial Cell Growth Factor (VEGFR) and Platelet Derived Growth Factor (PDGFR) expressed on tumor cells or vascular endothelial cells [3,4]. The blood perfusion reductions can be observed preceding tumor size reduction after lenvatinib therapy due to its anti-angiogenic effect.

A patient's response to cancer therapy is usually evaluated using the modified Response Evaluation Criteria in Solid Tumors (mRECIST) criteria [5]. Contrast-enhanced computed tomography and Magnetic Resonance Imaging (MRI) are the conventional imaging modalities for evaluating the size and blood flow of HCCs, but contrast media are difficult to use in patients with renal failure or allergies.

Diffusion-Weighted Imaging (DWI) is obtained by visualizing the Brownian motion of water molecules and is used to diagnose various tumors. The Apparent Diffusion Coefficient (ADC), calculated by DWI, is an indicator of water molecule diffusion, which helps assess the tumor malignancy grade. Furthermore, DWI reflects not only water molecule diffusion but also microcirculation. Intravoxel Incoherent Motion (IVIM) is an advanced technique using multi-b-value DWI with bi-exponential curve fitting that can separately evaluate water molecule diffusion and microcirculation. Reports indicate that IVIM MRI is useful for the detailed diagnosis of prostate cancer and differential diagnosis of breast tumors [6-8]. A previous study also reported that IVIM MRI can be used to evaluate necrosis and viable tumor in HCC [9]. Therefore, we hypothesized that this imaging technique could help predict the treatment response to lenvatinib and assess its effects after treatment in patients with HCC.

Thus, this study evaluated associations between the early therapeutic outcomes of lenvatinib treatment for advanced HCC and DWI/IVIM MRI parameters.

Material and Methods

Participants

This prospective study was approved by the institutional ethics committee and written informed consent from patients was obtained. This study included patients receiving lenvatinib therapy for Barcelona Clinic Liver Cancer stage B or C HCC and who underwent IVIM MRI examinations from March to October 2019. Lenvatinib (Eisai, Tokyo, Japan) was given orally at either 8mg/day for the patients <60kg or 12mg/day for those ≧60kg. we included 20 patients, but two were excluded due to a lack of two-or six-week images, and two were excluded because of poor image quality due to artifacts. The final study population included 16 patients with HCC (Table 1 and Figure 1).

The curative effect was evaluated using mRECIST criteria [5]. After six weeks, the patients were divided into groups based on the curative effects: with progressive disease (PD): a ≥20% increase in the sum of diameters of enhancing target lesions or the appearance of new lesions; and without PD (non-PD; complete response, partial response, and stable disease). Clinical data were obtained from electronic medical records.

Table 1: Patient characteristics associated with lenvatinib treatment.

Characteristics	Non-PD (n = 9)	PD (n = 7)	P
Age (years; mean ± SD)	72.33 ± 7.75	70.71 ± 10.89	0.733
Sex			1.000
Men	8 (89%)	6 (86%)	
Women	1 (11%)	1 (14%)	
Cause of liver disease			0.260
Hepatitis B virus	3 (33%)	2 (28.5%)	
Hepatitis C virus	1 (11%)	3 (43%)	
Alcohol	3 (33%)	0 (0%)	
Undetermined	2 (23%)	2 (28.5%)	
AFP at baseline (ng/mL)	122.35±45.32	127.34±53.47	0.233
Histological differentiation			0.487
Well	0 (0%)	1 (14%)	
Moderate	7 (78%)	5 (72%)	
Poor	2 (22%)	1 (14%)	
BCLC staging classification			0.718
Stage A	0 (0%)	0 (0%)	
Stage B	7 (78%)	3 (43%)	
Stage C	2 (22%)	4 (57%)	
Stage D	0 (0%)	0 (0%)	
Target lesion size (i.e., largest tumor identified at baseline (mm; mean ± SD)			
Baseline	33.04 ± 23.89	45.31 ± 54.27	0.551
2 weeks	28.91 ± 23.58	47.31 ± 53.40	0.368
6 weeks	27.31 ± 23.04	53.47 ± 53.63	0.349
Hemorrhage			
Baseline	1 (11%)	1 (14%)	1.000
2 weeks	2 (22%)	2 (29%)	1.000
6 weeks	2 (22%)	2 (29%)	1.000
Necrosis			
Baseline	1 (11%)	2 (29%)	0.550
2 weeks	2 (22%)	2 (29%)	1.000
6 weeks	2(22%)	2 (29%)	1.000

BCLC: Barcelona Clinic Liver Cancer; PD: Progressive Disease; AFP: Alpha Fetoprotein; SD: Standard Deviation.

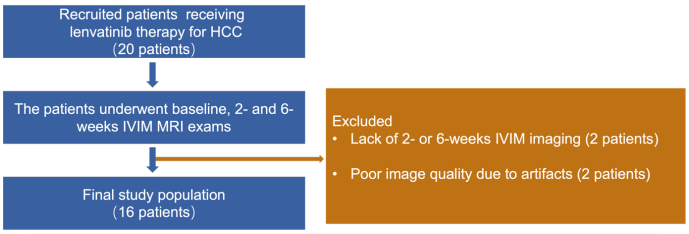

Figure 1: Flow diagram of the study population.

IVIM: Intravoxel Incoherent Motion; HCC: Hepatocellular Carcinoma; MRI: Magnetic Resonance Imaging.

IVIM MRI protocol

A liver MRI examination was performed within one week before starting lenvatinib therapy (baseline) and after two and six weeks. MRI exams were performed using a 3.0-Tesla scanner with 16 channel body coil (Ingenia, Philips Healthcare, Best, the Netherlands). DWI was acquired using the following sequence parameters: spin-echo echo-planar imaging; Repetition Time (TR), 1134 ms; Echo Time (TE), 143 ms; flip angle, 90°; matrix size, 128 × 128; field of view, 36 × 36 cm; 1 averaging; slice thickness, 6 mm; receiver bandwidth, 921 Hz/pixel; fat suppression; spectral presaturation with inversion recovery; acquisition time, 20 s; b-values: 0, 10, 30, 50, 100, 200, 400, 800, 1000, 1500, and 2000 s/mm^2. DWI was performed while the patient held their breath.

Fat suppressed three-dimensional spoiled gradient-recalled echo T1-weighted sequences (TR/TE=3.0/1.5 ms; flip angle, 10^O; field of view, 36 × 36 cm; matrix, 288 × 231, slice thickness 4.2 mm) were scanned. Dynamic MRI was performed using gadolinium-ethoxybenzyl-diethylenetriamine pentaacetic acid (Primovist; Bayer AG, Berlin, Germany). The contrast medium (0.025 mmol/kg) was injected at 1.0 mL/s. The arterial phase (AP) timing was determined using the test injection method, defined as the time at which the abdominal aorta reached a peak of +10 s.

DWI/IVIM MRI parameters and Enhancement Ratio (ER) calculations

All IVIM-DWI images were transferred to a workstation for postprocessing; the program was an offline prototype software provided by the Magnetic Resonance (MR) scanner vendor (Philips Healthcare).

The biexponential model from an IVIM-DWI sequence was expressed using the following equation according to Le Bihan et al [10].

The ADC value was calculated using a mono-exponential model using b = 0 and 800 s/mm^2 as follows:

$$S\,I_b/S\,I_0 = \exp\,-(b)\,\times\,ADC$$

Where SI_0 represents the signal intensity without diffusion weighting, and SI_b represents the signal intensity with diffusion weighting.

Furthermore, the IVIM-DWI parameters were generated using a bi-exponential model as follows:

$$SI_b/SI_0 = \left(F_{perfusion} \times \exp(-b) \times D^*\right) + \left(F_{diffusion} \times \exp(-b) \times DC\right)$$

Where D* is the pseudo diffusion coefficient, DC is the true diffusion coefficient, $F_{perfusion}$ (PF) is the perfusion fraction, SI is the signal intensity for a selected b-value, and SI_0 is the signal intensity for b = 0 s/mm^2. The b-value is the diffusion sensitivity coefficient.

We used the segment analysis method described previously to avoid mathematical instability when three IVIM-DWI parameters were simultaneously fitted. Since blood flow perfusion is negligible at high b-values, the DC values were obtained using a mono-exponential model with b-values of >200 s/mm^2. D* and PF were then fitted using the bi-exponential model when the b-value was low (<200 s/mm^2).

First, the mean SIs of the Region of Interest (ROI) in the largest tumor (i.e., the target lesion) were evaluated by two observers (observer 1 and observer 2; with 9 and 19 year's experience, respectively). The average values of two observers were used for analysis. The therapeutic response was evaluated using dynamic MRI examinations with IVIM analysis at baseline and after two and six weeks of lenvatinib treatment. Then, to differentiate the effect of each component within the tumors based on SI, the tumor component signals were separately measured. Viable tumor components were defined as solid lesions with significant enhancement in the Arterial Phase (AP), hemorrhagic tumor components were areas with high SI in the precontrast T1 weighted image, and necrotic tumor components were areas with no enhancement in each phase on Dynamic Contrast-Enhanced (DCE) MR images.

Additionally, relative Enhancement Ratios (ERs) were calculated in the HCC based on dynamic APs in the largest tumor using the following formula [9]:

$$ER = \frac{\left(SI_{post} - SI_{pre}\right)}{SI_{pre}}$$

Where SI_{post} is the mean SI measured on the AP images, and SI_{pre} is the mean SI measured on unenhanced images.

Statistical analyses

The descriptive data expressed as means ± standard deviations for continuous variables and number (%) for categorical variables. Two-sample t test for continuous variables and Fisher's exact test or chi square test were used for categorical variables. The DWI/IVIM MRI parameters are expressed as means ± standard deviations. DWI/IVIM MRI parameter and ER differences between the PD and non-PD groups were analyzed by two-sample t test. DWI/IVIM MRI parameter differences between the HCC viable lesions, hemorrhagic, and necrotic tumor components were analyzed by paired-sample Student's t-test. DWI/IVIM MRI parameter differences before and after treatment were evaluated using the Friedman test. A P-value less than 0.05 was considered statistically significant. Spearman's rank correlations were performed using the DWI/IVIM MRI parameters and ERs in the HCC tumors. Cutoff values were determined by a Receiver Operating Characteristic (ROC) curve analysis, and the sensitivity and specificity of DWI/IVIM MRI parameters and ERs were calculated for variables with significant differences. Intraclass Correlation Coefficient (ICC) of two observers was evaluated. All statistical analyses were performed using SPSS Statistics software (version 22, SPSS, IBM Corporation, Armonk, NY, USA).

Results

Demographic and clinical information

We included seven patients in the PD group and nine in the non-PD group (complete response, n=4; stable disease, n=5); Table 1 presents detailed patient information. The target lesion sizes were comparable between the PD and non-PD groups (P=0.55), although the lesions in the PD group were larger.

DWI/IVIM MRI parameters and ERs: non-PD vs. PD

The Intra-Class Correlation Coefficient (ICC) values between the two observers were 0.654~0.968, which indicated substantial or excellent inter-observer agreement in the measurements between the two observers.

At baseline, the ADCs were significantly lower (P=0.007) in the non-PD group (0.98 ± 0.08) than in the PD group (1.16 ± 0.14) but significantly higher after six weeks of treatment (non-PD, 1.27 ± 0.1; PD, 1.14 ± 0.11; P=0.031).

At baseline, the DCs were significantly lower (P=0.018) in the non-PD group (0.96 ± 0.15) than in the PD group (1.14 ± 0.12); At six weeks, the DCs were significantly higher in the non-PD group than in the PD group (non-PD, 1.25 ± 0.19; PD, 0.96 ± 0.23; P=0.016).

The D* and PF values did not significantly differ between the PD and non-PD groups at any point. The ER AP was significantly lower (P=0.003) in the non-PD group (0.23 ± 0.20) than in the PD group (0.75 ± 0.29) after six weeks of treatment (Table 2, Figures 2 and 3).

Table 2: Diffusion weighted imaging, intravoxel incoherent motion magnetic resonance imaging parameters and enhancement ratios of patients with and without PD.

Parameter	Period	Non-PD	PD	P value (Non-PD vs PD)	ICC
ADC (10^{-3} mm^2/s)	Baseline	0.98 ± 0.08	1.16 ± 0.14	0.007	0.888
	2 weeks	1.16 ± 0.13	1.18 ± 0.08	0.648	
	6 weeks	1.27 ± 0.1	1.14 ± 0.11	0.031	
P value (Baseline vs 6 weeks)		<0.001	0.835		
DC (10^{-3} mm^2/s)	Baseline	0.96± 0.15	1.14 ± 0.12	0.018	0.968
	2 weeks	1.08 ± 0.18	0.92 ± 0.17	0.101	
	6 weeks	1.25 ± 0.19	0.96 ± 0.23	0.016	
P value (Baseline vs 6 weeks)		0.003	0.081		
D* (10^{-3} mm^2/s)	Baseline	45.32 ± 24.99	46.67 ± 25.34	0.917	0.867
	2 weeks	49.81 ± 22.43	44.54 ± 20.96	0.639	
	6 weeks	49.43 ± 20.39	70.46 ± 45.15	0.231	
P value (Baseline vs 6 weeks)		0.707	0.248		
PF (%)	Baseline	0.22± 0.12	0.29 ± 0.06	0.208	0.654
	2 weeks	0.21 ± 0.11	0.20 ± 0.07	0.826	
	6 weeks	0.20 ± 0.10	0.25 ± 0.08	0.285	
P value (Baseline vs 6 weeks)		0.678	0.357		
ER AP	Baseline	0.82 ± 0.29	0.83 ± 0.23	0.864	0.762
	2 weeks	0.21 ± 0.17	0.44 ± 0.35	0.160	
	6 weeks	0.23 ± 0.20	0.75 ± 0.29	0.003	
P value (Baseline vs 6 weeks)		<0.001	0.562		

ADC: Apparent Diffusion Coefficient; D*: Pseudo-Diffusion Coefficient; DC: True Diffusion Coefficient; ER AP: Enhancement Ratio in the Arterial Phase; ICC: Intraclass Correlation Coefficient; PD: Progressive Disease; PF: Perfusion Fraction.

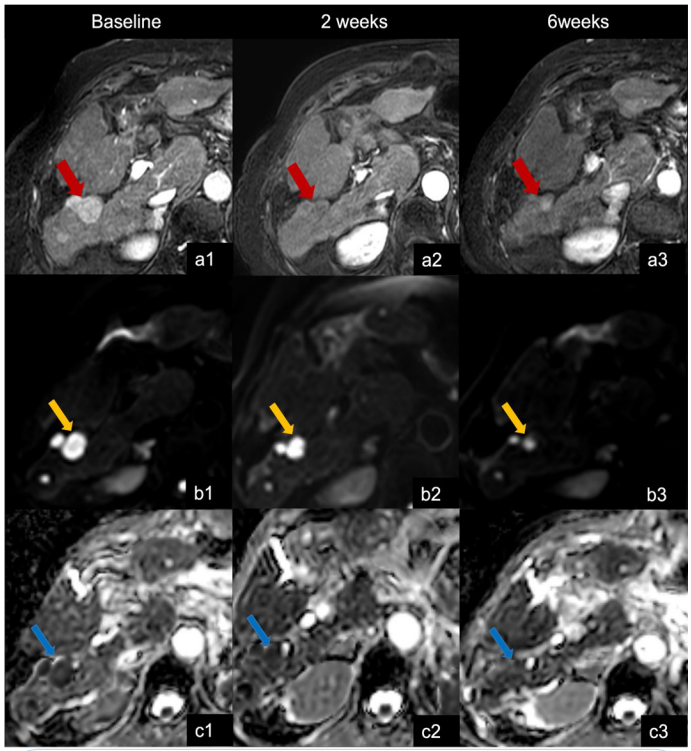

Figure 2: Representative images from a 60-year-old man with advanced hepatocellular carcinoma who showed partial response by lenvatinib treatment.

After lenvatinib treatment, the tumor size decreased from 25 mm at baseline to 20 mm after two weeks and to 15 mm after six weeks. (a) Gadoxetate-enhanced T1-weighted AP images show a hypervascular nodule in S6 of the liver (red arrows) that becomes less enhanced after lenvatinib treatment. The enhancement ratio in the arterial phase decreased from 0.39 to 0.27. (b) Diffusion-weighted images (b-value = 800 s/mm^2) show a hyperintense nodule at baseline (yellow arrows) with decreasing signal intensity after treatment. (c) From baseline to six weeks, the apparent diffusion coefficient increased from 0.99 to 1.38 (10^{-3} mm^2/s) (blue arrows), the true diffusion coefficient increased from 0.93 to 1.04 (10^{-3} mm^2/s).

DWI/IVIM MRI parameters and ERs: baseline vs. six weeks of lenvatinib treatment

In the PD group, changes in ADC and DC were statistically insignificant (ADC: baseline, 1.16 ± 0.14; six weeks, 1.14 ± 0.11; P=0.835; DC: baseline, 1.14 ± 0.12; six weeks, 0.96 ± 0.23; P=0.081). In the non-PD group, ADC and DC were significantly increased after treatment relative to baseline (ADC: baseline, 0.98 ± 0.08; six weeks, 1.27 ± 0.1; P <0.001; DC: baseline, 1.14 ± 0.12; six weeks, 0.96 ± 0.23; P=0.003). The D* and PF values did not differ between baseline and 6 weeks both in the PD and non-PD groups. Finally, the ER AP significantly decreased from baseline to six weeks in the non-PD group (ER AP: baseline, 0.82 ± 0.29; six weeks, 0.23 ± 0.20; P <0.001; Table 2 and Figure 4).

DWI/IVIM MRI parameters in viable, hemorrhage, and necrotic tumor components after six weeks of lenvatinib treatment

The hemorrhagic areas (ADC, 0.64 ± 0.09; DC, 0.71 ± 0.11) had significantly lower ADCs and DCs than the viable areas (ADC, 1.03 ± 0.10; DC, 1.13 ± 0.14; both P <0.001). However, the necrotic areas (ADC, 1.65 ± 0.13; DC, 1.34 ± 0.07) had significantly higher ADCs and DCs than the viable areas (ADC, 1.03 ± 0.10; DC, 1.13 ± 0.14; both P <0.001; Table 3).

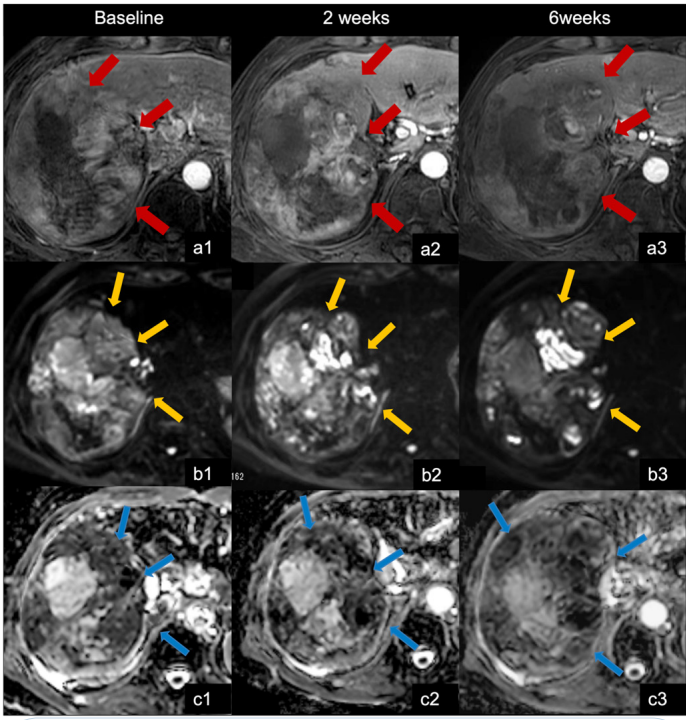

Figure 3: Representative images from a 50-year-old-man with advanced hepatocellular carcinoma who showed progressive disease after lenvatinib treatment.

The tumor maximum diameter increased from baseline (144 mm) to two weeks (150 mm) and six weeks (174 mm) after lenvatinib treatment. (a) Gadoxetate-enhanced T1-weighted arterial phase images show an unevenly hyperintense giant mass in the right lobe of the liver (thick red arrow). The enhancement ratio in the arterial phase decreased from 0.61 to 0.45. (b) Diffusion-weighted images (b-value = 800 s/mm^2) show a hyperintense mass (yellow arrows). (c) At baseline, two, and six weeks, the apparent diffusion coefficients (ADC) were 0.97, 1.24, and 1.03 (10^{-3} mm^2/s) (blue arrows), respectively, and the true diffusion coefficients (DC) were 1.20, 1.27, and 1.24 (10^{-3} mm^2/s), respectively. Large patchy necrotic areas were seen in the tumor, which showed higher ADC and higher DC than viable tumor in 6 weeks (1.48 and 1.33 (10^{-3} mm^2/s), respectively).

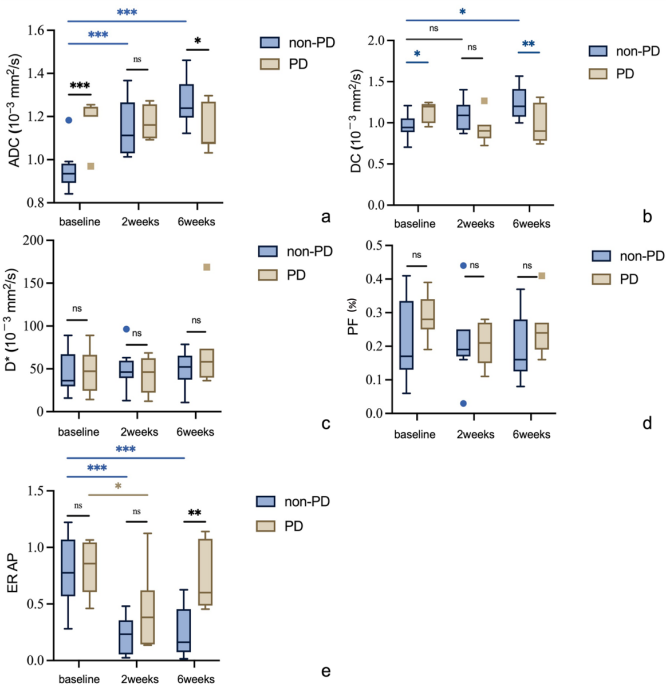

Figure 4: Diffusion weighted image, intravoxel incoherent motion magnetic resonance imaging parameters and enhancement ratio in the arterial phase comparisons between patients with and without progressive disease.

(a) The baseline ADC values were significantly lower in the non-PD group than in the PD group, and the ADC values significantly increased from baseline to six weeks after treatment in the non-PD group. (b) The baseline DC values were significantly lower in the non-PD group than in the PD group, and the DC values significantly increased from baseline to six weeks after treatment in the non-PD group The (c) D* and (d) PF values did not differ between the groups or time points. (e) The six-week ER AP value was significantly lower in the non-PD group than in the PD group. In the non-PD group, the ER AP value significantly decreased from baseline to six weeks after treatment. In the PD group, the ER AP value significantly decreased only after two weeks.

ADC: Apparent Diffusion Coefficient; D*: Pseudo Diffusion Coefficient; DC: True Diffusion Coefficient; ER AP: Enhancement Ratio in the Arterial Phase; ns: not significant; PD: Progressive Disease; PF: Perfusion Fraction. * P <0.05; ** P <0.01; *** P <0.001.

Table 3: Diffusion weighted imaging and intravoxel incoherent motion magnetic resonance imaging parameters six weeks after lenvatinib in viable, hemorrhagic, and necrotic tumor components.

Parameters	Viable HCC	Hemorrhage	P value
ADC (10^{-3} mm^2/s)	1.03 ± 0.10	0.64 ± 0.09	<0.001
DC (10^{-3} mm^2/s)	1.13 ± 0.14	0.71 ± 0.11	<0.001
D* (10^{-3} mm^2/s)	51.97 ± 24.4	46.51 ± 25.66	0.615
PF (%)	0.27 ± 0.11	0.23 ± 0.11	0.053
	Viable HCC	**Necrosis**	**P value**
ADC (10^{-3} mm^2/s)	1.03 ± 0.10	1.65 ± 0.13	<0.001
DC (10^{-3} mm^2/s)	1.13 ± 0.14	1.34 ± 0.07	<0.001
D* (10^{-3} mm^2/s)	51.97 ± 24.4	39.33 ± 19.44	0.088
PF (%)	0.27 ± 0.11	0.24 ± 0.26	0.562

ADC: Apparent Diffusion Coefficient; D*: Pseudo-Diffusion Coefficient; DC: True Diffusion Coefficient; HCC: Hepatocellular Carcinoma; PF: Perfusion Fraction.

Table 4: Receiver operating characteristic curve analyses for differentiating between patients with and without progressive disease using the baseline diffusion weighted imaging, intravoxel incoherent motion magnetic resonance imaging parameters and enhancement ratios.

Parameters	Cutoff value	AUC (95%CI)	Sensitivity (%)	Specificity (%)
ADC (10^{-3} m^2/s)	1.191	0.825 (0.596, 1.000)	71.4	88.9
DC (10^{-3} mm^2/s)	0.986	0.865 (0.684, 1.000)	71.4	77.8
D* (10^{-3} mm^2/s)	42.300	0.500(0.196, 0.804)	0.000	100
PF (%)	0.180	0.690 (0.414, 0.967)	28.6	66.7
ER AP	0.725	0.492 (0.196, 0.788)	71.4	55.6

ADC: Apparent Diffusion Coefficient; AUC: Area Under the Curve; D*: Pseudo-Diffusion Coefficient; DC: True Diffusion Coefficient; ER AP: Enhancement Ratio in the Arterial Phase; PF: Perfusion Fraction.

DWI/IVIM MRI parameter and ER correlations

At baseline, correlations were not identified between the IVIM MRI parameters and the liver ERs (ADC: r=0.028, P=0.919; DC: r=-0.026, P=0.934; D*: r=-0.094, P=0.009; PF: r=0.394, P=0.132; Figure 5a)

ROC curves of the DWI/IVIM parameters and ERs at baseline for predicting PD

The cutoff value and subsequent sensitivity and specificity values for ADC were 1.191 (10^{-3} mm^2/s), 71%, and 89% (95% Confidence Interval [CI]: 0.596, 1.000). The cutoff value and subsequent sensitivity and specificity values for DC were 0.986 (10^{-3} mm^2/s), 71%, and 78% (95% CI: 0.684, 1.000; Table 4 and Figure 5b).

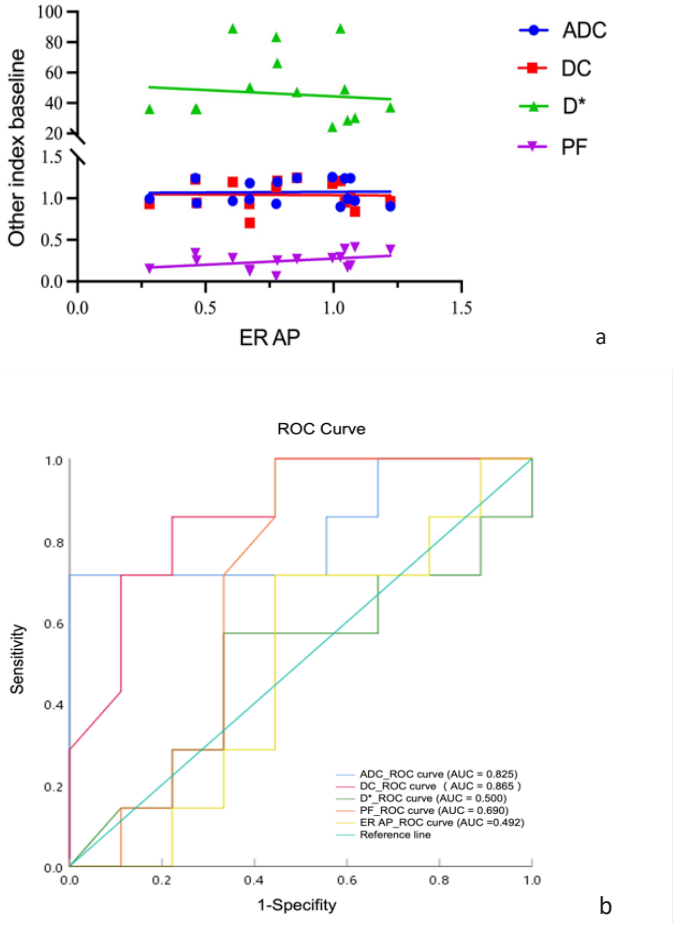

Figure 5: Correlations between diffusion weighted imaging, intravoxel incoherent motion magnetic resonance imaging parameters and enhancement ratio at baseline, and receiver operating characteristic curves for differentiating between patients with and without progressive disease.

(a) No significant correlation was seen between IVIM MRI parameters and the liver ERs. (b) The ADC cutoff value was 1.191 (10^{-3} mm^2/s) with 71% sensitivity and 89% specificity (AUC=0.825, 95% CI: 0.596, 1.000). The DC cutoff value was 0.986 (10^{-3} mm^2/s) with 71% sensitivity and 78% specificity (AUC=0.865, 95% CI: 0.684, 1.000).

ADC: Apparent Diffusion Coefficient; AUC: Area Under the Curve; CI: Confidence Interval; DC: True Diffusion Coefficient; D*: Pseudo Diffusion Coefficient; DWI: Diffusion Weighted Imaging; ER AP: Enhancement Ratio in the Arterial Phase; IVIM: Intravoxel Incoherent Motion; PF: Perfusion Fraction; ROC: Receiver Operating Characteristic.

Discussion

We found that baseline ADCs and DCs were significantly lower in the non-PD group than in the PD group, suggesting that therapeutic outcome predictions before initiating treatment is possible. Furthermore, the DC's AUC was higher than that of the ADC for predicting treatment outcomes. Previous reports indicate that the HCC's histological grade correlates more strongly with the DC than with the ADC, and the DC of patients with high-grade HCC is significantly lower than that of patients with low-grade HCC [11]. However, unlike the DC value, the ADC value includes the pure diffusion and perfusion measurements; thus, interpreting ADC results may be complicated. In our study, moderate and poor differentiation was more prevalent in the non-PD group than in the PD group. Previous studies have also reported favorable treatment results in patients with histologically poorly differentiated tumors [12,13]. In addition, the lenvatinib target of VEGFR and FGFR expression level are higher in poorly differentiated HCC and related with poor prognosis [14,15], which is consistent with our result that non-PD group after lenvatinib showed lower baseline ADC and DC.

Moreover, the ADC and DC values increased from the baseline value after treatment in the non-PD group. Therefore, ADC and DC help predict the treatment response and evaluate the outcome. This result may be because microscopic necrosis and intercellular structural alterations after the treatment caused significantly higher ADC and DC values [9,16]; anti-proliferative and anti-angiogenic treatments induce cell necrosis and cell collapse, resulting in expansion of the extracellular space and thus loss of diffusion restriction. We observed necrosis in 33% of patients in the non-PD group after lenvatinib treatment. In contrast, in the PD group, 43% of patients had tumor necrosis at baseline and 14% developed necrosis after treatment.

Conversely, hemorrhage decreases the ADC values [17]. In our study, hemorrhage was observed in both groups after treatment. However, compared with large areas of necrosis, the hemorrhagic areas were mainly patchy and circumscribed. Likely, the bleeding and necrosis processes partially overlap, perhaps partly compensating for the expected changes in ADC and DC. The ADC and DC increases in patients without PD were likely because the effects of tumor necrosis dominate those of intra-tumor hemorrhage [18]. Also, the b-value choice affects the ADC value, and differences in the distribution of low b-values would cause ADC changes [19,20]. Therefore, the DC value is more stable than the ADC value.

The D* and PF values did not differ between the non-PD and PD groups. However, studies have reported increased PF values after two weeks of treatment, surmising that lenvatinib inhibits tumor angiogenesis, causing disruption and normalization of tumor vessels [21]. Tumor blood vessel normalization suppresses permeability, decreasing the pressure of the tumor tissue. The increased PF value reflects an increase in the perfusion rate by the normalization of tumor blood vessels. However, it has been reported that the D* and PF values have poor reproducibility [22].

Patients without PD also had a significantly greater decrease in AP enhancement than those with PD in our study, similar to previous research [23]. However, we did not observe a significant correlation between IVIM MRI parameters and the ER AP. Some have reported a positive correlation between PF and ER AP in HCC [11], while others reported no correlation in the liver parenchyma between IVIM and DCE-MRI parameters [24].

IVIM provides intravascular information about capillary vessels, whereas DCE-MRI provides perfusion information (including extravascular information) and has a larger time scale. Previous studies have suggested that IVIM MRI does not measure tissue perfusion as well as DCE-MRI [25], which is more sensitive to the amount of blood passing through voxels. Therefore, we hypothesized that perfusion in IVIM MRI would be more sensitive for assessing tumor microvascular perfusion after multikinase inhibitor treatment. However, our results were different than expected, perhaps because of the opposite effects on the PF values between normalized tumor blood vessels and decreased blood supply after treatment in the non-PD group.

Our study had several limitations. First, we included a small number of patients; thus, we need to accumulate more cases and validate our results. Second, some cases showed poor IVIM MRI fitting, and outliers were removed from the measurements when such cases occurred. In other studies, scanning using the appropriate b-values and other techniques, such as Bayesian fitting, have been used to obtain better fitting. Therefore, future studies should test other methods to improve fitting [22,26,27].

Conclusions

Our results suggest that the ADC and DC values obtained by DWI/IVIM MRI are useful biomarkers for predicting and evaluating the therapeutic effects of lenvatinib for HCC.

Declarations

Author contributions

All authors conceived the study and participated in its design and coordination. Y. Z. and A.K. performed the image and statistical analyses. All authors have read and approved the final manuscript.

Data availability statement

The original contributions presented in the study are included in the article and further inquiries can be directed to the corresponding authors.

Funding

No funding was received.

Declarations Conflict of interest

The authors declare that the research was conducted without commercial or financial relationships that could be construed as potential conflicts of interest.

Ethical approval

This study was approved by institutional review board.

Informed consent

Written informed consent was obtained from all patients.

Acknowledgement

We are grateful to Dr. Yu Ueda of Philips Healthcare for his technical support.

References

1. McGlynn KA, Petrick JL, El-Serag HB. Epidemiology of Hepatocellular Carcinoma. Hepatology. 2021; 73: 4-13.

2. Oranratnachai S, Rattanasiri S, Pooprasert A, Tansawet A, Reungwetwattana T, et al. Efficacy of First Line Systemic Chemotherapy and Multikinase Inhibitors in Advanced Hepatocellular Carcinoma: A Systematic Review and Network Meta-Analysis. Front Oncol. 2021; 11: 654020

3. Kato Y, Tabata K, Kimura T, Yachie-Kinoshita A, Ozawa Y, et al. Lenvatinib plus anti-PD-1 antibody combination treatment activates CD8+ T cells through reduction of tumor-associated macrophage and activation of the interferon pathway. PLoS One. 2019; 14: e0212513.

4. Torrens L, Montironi C, Puigvehi M, Mesropian A, Leslie J, et al. Immunomodulatory Effects of Lenvatinib Plus Anti-Programmed Cell Death Protein 1 in Mice and Rationale for Patient Enrichment in Hepatocellular Carcinoma. Hepatology. 2021; 74: 2652-2669.

5. Llovet JM, Lencioni R. mRECIST for HCC: Performance and novel refinements. J Hepatol. 2020; 72: 288-306.

6. Kawashima H, Miyati T, Ohno N, Ohno M, Inokuchi M, et al. Differentiation Between Luminal-A and Luminal-B Breast Cancer Using Intravoxel Incoherent Motion and Dynamic Contrast-Enhanced Magnetic Resonance Imaging. Acad Radiol. 2017; 24: 1575-1581.

7. Kawashima H, Miyati T, Ohno N, Ohno M, Inokuchi M, et al. Differentiation between phyllodes tumours and fibroadenomas using intravoxel incoherent motion magnetic resonance imaging: Comparison with conventional diffusion-weighted imaging. Br J Radiol. 2018; 91: 20170687.

8. Ueda Y, Takahashi S, Ohno N, Kyotani K, Kawamitu H, et al. Tri-exponential function analysis of diffusion-weighted MRI for diagnosing prostate cancer. J Magn Reson Imaging. 2016; 43: 138-148.

9. Kakite S, Dyvorne HA, Lee KM, Jajamovich GH, Knight-Greenfield A, et al. Hepatocellular carcinoma: IVIM diffusion quantification for prediction of tumor necrosis compared to enhancement ratios. Eur J Radiol Open. 2016; 3: 1-7.

10. Le Bihan D, Breton E, Lallemand D, ML Aubin, J Vignaud, et al. Separation of diffusion and perfusion in intravoxel incoherent motion MR imaging. Radiology. 1988; 168: 497-505.

11. Woo S, Lee JM, Yoon JH, Joo I, Han JK, et al. Intravoxel incoherent motion diffusion-weighted MR imaging of hepatocellular carcinoma: Correlation with enhancement degree and histologic grade. Radiology. 2014; 270: 758-767.

12. Rodríguez-Hernández MA, Chapresto-Garzón R, Cadenas M, Elena Navarro-Villarán, María Negrete, Miguel A. Gómez-Bravo, et al. Differential effectiveness of tyrosine kinase inhibitors in 2D/3D culture according to cell differentiation, p53 status and mitochondrial respiration in liver cancer cells. Cell Death Dis. 2020; 11: 339.

13. Sasaki R, Kanda T, Fujisawa M, Matsumoto N, Masuzaki R, et al. Different Mechanisms of Action of Regorafenib and Lenvatinib on Toll-Like Receptor-Signaling Pathways in Human Hepatoma Cell Lines. Int J Mol Sci. 2020; 21.

14. Amaoka N, Saio M, Nonaka K, Imai H, Tomita H, et al. Expression of vascular endothelial growth factor receptors is closely related to the histological grade of hepatocellular carcinoma. Oncol Rep. 2006; 16: 3-10.

15. Jun BG, Lee WC, Jang JY, Jeong SW, Chang Y, et al. Relation of fibroblast growth factor receptor 2 expression to hepatocellular carcinoma recurrence after liver resection. PLoS One. 2020; 15: e0227440.

16. Koh DM, Scurr E, Collins D, Kanber B, Norman A, et al. Predicting response of colorectal hepatic metastasis: Value of pretreatment apparent diffusion coefficients. AJR Am J Roentgenol.

2007; 188: 1001-1008.

17. Atlas SW, DuBois P, Singer MB, Lu D. Diffusion measurements in intracranial hematomas: Implications for MR imaging of acute stroke. AJNR Am J Neuroradiol. 2000; 21: 1190-1194.

18. Silvera S, Oppenheim C, Touze E, Ducreux D, Philippe P, et al. Spontaneous intracerebral hematoma on diffusion-weighted images: Influence of T2-shine-through and T2-blackout effects. AJNR Am J Neuroradiol. 2005; 26: 236-241.

19. Le Bihan D. Intravoxel incoherent motion perfusion MR imaging: A wake-up call. Radiology. 2008; 249: 748-752.

20. Yamaguchi R, Yano H, Iemura A, Ogasawara S, Haramaki M, et al. Expression of vascular endothelial growth factor in human hepatocellular carcinoma. Hepatology. 1998; 28: 68-77.

21. Shirota N, Saito K, Sugimoto K, Takara K, Moriyasu F, et al: Intravoxel incoherent motion MRI as a biomarker of sorafenib treatment for advanced hepatocellular carcinoma: A pilot study. Cancer Imaging. 2016; 16: 1.

22. Andreou A, Koh DM, Collins DJ, Blackledge M, Wallace T, et al. Measurement reproducibility of perfusion fraction and pseudodiffusion coefficient derived by intravoxel incoherent motion diffusion-weighted MR imaging in normal liver and metastases. Eur Radiol. 2013; 23: 428-434.

23. Salvaggio G, Furlan A, Agnello F, Cabibbo G, Marin D, et al. Hepatocellular carcinoma enhancement on contrast-enhanced CT and MR imaging: Response assessment after treatment with sorafenib: Preliminary results. Radiol Med. 2014; 119: 215-221.

24. Patel J, Sigmund EE, Rusinek H, Oei M, James SB, et al. Diagnosis of cirrhosis with intravoxel incoherent motion diffusion MRI and dynamic contrast-enhanced MRI alone and in combination: preliminary experience. J Magn Reson Imaging. 2010; 31: 589-600.

25. Henkelman RM: Does IVIM measure classical perfusion? Magn Reson Med. 1990; 16: 470-475.

26. Luciani A, Vignaud A, Cavet M, Jeanne Tran VN, Mallat A, et al. Liver cirrhosis: Intravoxel incoherent motion MR imaging--pilot study. Radiology. 2008; 249: 891-899.

27. Neil JJ, Bretthorst GL. On the use of Bayesian probability theory for analysis of exponential decay data: An example taken from intravoxel incoherent motion experiments. Magn Reson Med. 1993; 29: 642-647.